Pharmacokinetic tuning of protein–antigen fusions enhances the immunogenicity of T-cell vaccines

Naveen K. Mehta[1,2], Roma V. Pradhan[2], Ava P. Soleimany [1,3], Kelly D. Moynihan[1,2,4],
Adrienne M. Rothschilds[1,2], Noor Momin [1,2], Kavya Rakhra[1], Jordi Mata-Fink[4,5],
Sangeeta N. Bhatia[1,2,6,7,8,9,11], K. Dane Wittrup [1,2,5 ✉] and Darrell J. Irvine [1,2,4,10,11 ✉]

[1]Koch Institute for Integrative Cancer Research, Massachusetts Institute of Technology, Cambridge, MA, USA. [2]Department of Biological Engineering, Massachusetts Institute of Technology, Cambridge, MA, USA. [3]Harvard Graduate Program in Biophysics, Harvard University, Boston, MA, USA. [4]The Ragon Institute of Massachusetts General Hospital, Massachusetts Institute of Technology and Harvard University, Cambridge, MA, USA. [5]Department of Chemical Engineering, Massachusetts Institute of Technology, Cambridge, MA, USA. [6]Harvard–MIT Health Sciences and Technology Program, Institute for Medical Engineering and Science, Massachusetts Institute of Technology, Cambridge, MA, USA. [7]Department of Electrical Engineering and Computer Science, Massachusetts Institute of Technology, Cambridge, MA, USA. [8]Department of Medicine, Brigham and Women's Hospital, Harvard Medical School, Boston, MA, USA. [9]Broad Institute of Massachusetts Institute of Technology and Harvard, Cambridge, MA, USA. [10]Department of Materials Science and Engineering, Massachusetts Institute of Technology, Cambridge, MA, USA. [11]Howard Hughes Medical Institute, Cambridge, MA, USA. ✉e-mail: wittrup@mit.edu; djirvine@mit.edu
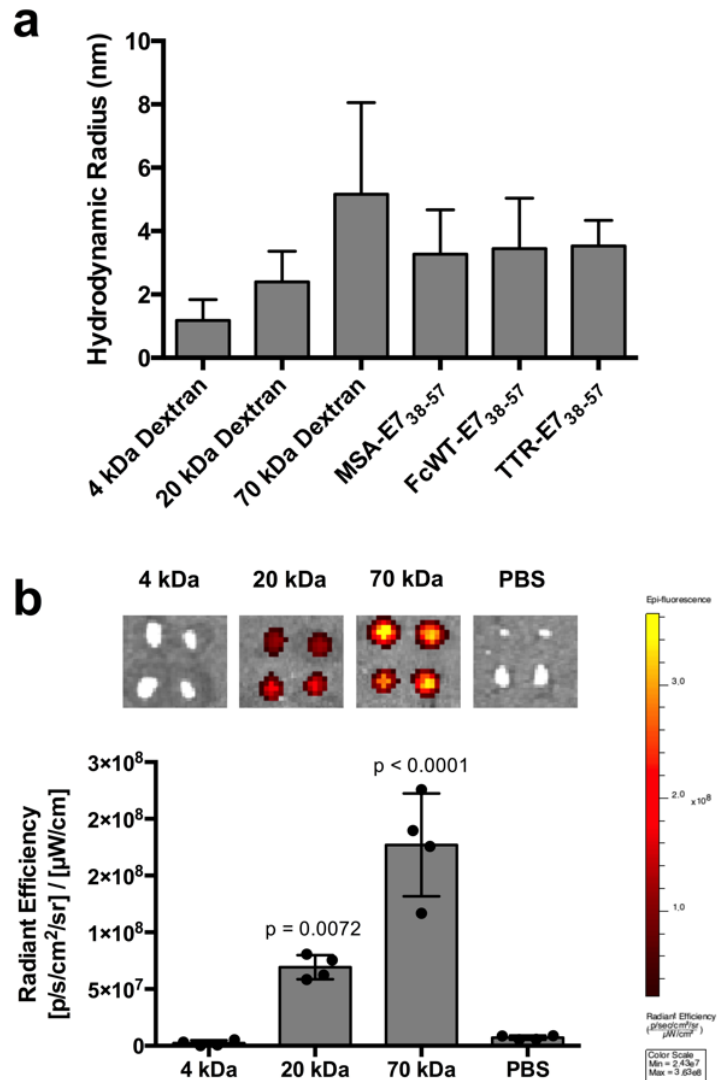
Supplementary Figure 1 Lymph node uptake is directly related to molecular weight.

(a) Shown are hydrodynamic radii of dextran and the indicated protein fusions were quantified on DLS (calculated fit ± SD, n=10 technical replicates). **(b)** Equimolar doses of FITC-dextran with the indicated molecular weight were injected subcutaneously in mice. 8 hours later, inguinal lymph nodes were excised and imaged on IVIS (mean ± SD, n = 4 lymph nodes per group). Statistical analysis calculated using one-way ANOVA with Dunnett's multiple comparisons test against PBS **(b)**.

a MSA-E7$_{38-57}$

b TTR-E7$_{38-57}$

c FcWT-E7$_{38-57}$
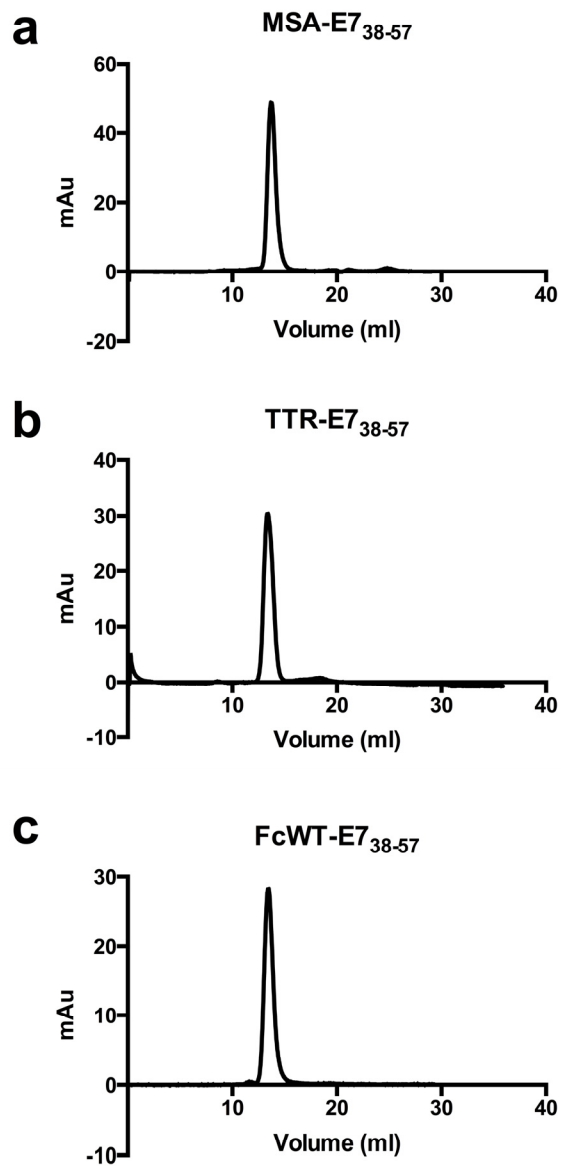
Supplementary Figure 2 Protein-antigen fusion constructs run as single peaks in size exclusion chromatography **(a-c)** SEC plots of the indicated protein-antigen fusion. 50 μg of protein were run in PBS on an analytical Superdex 200 Increase column.
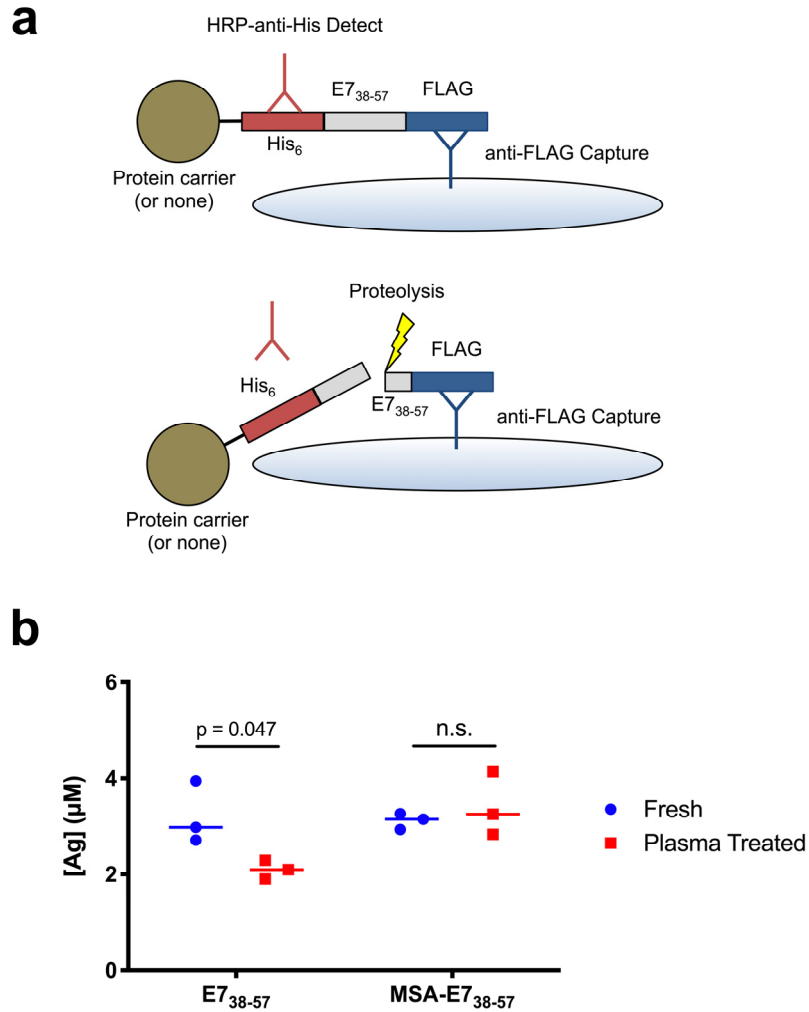
Supplementary Figure 3 Direct test of proteolytic stability. **(a)** Schematic of the sandwich ELISA used to assess proteolytic stability. Following plasma incubation, mixed reaction was incubated with ELISA plates coated with anti-FLAG capture antibody. Detection was performed with an HRP-conjugated anti-His antibody. **(b)** His-$E7_{38-57}$-FLAG or MSA-His-$E7_{38-57}$-FLAG was incubated in fresh 20% mouse plasma for 4 hours. Intact antigen concentration was quantified via sandwich ELISA with FLAG capture and His detection (n = 3 replicates). Data are representative of two independent experiments. Statistical significance calculated using two-tailed t tests between groups on the x-axis with Holm-Sidak multiple comparisons test **(b)**.
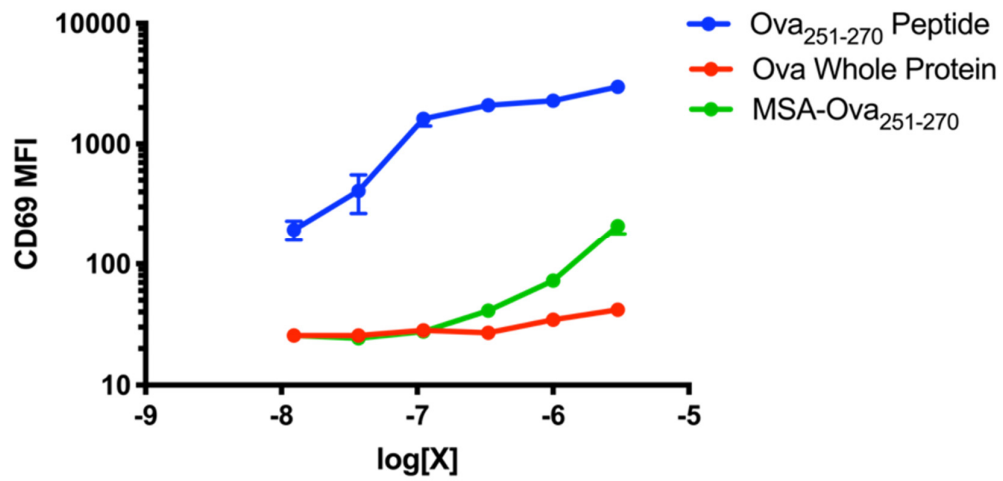
Supplementary Figure 4 MSA-epitope fusions are better processed than whole protein antigen. Splenocytes from OTI mice were cultured with the indicated antigenic constructs for 24 hours. After incubation, CD8+ T cells were assessed for CD69 expression by flow cytometry (mean ± SEM, n = 2 replicates).
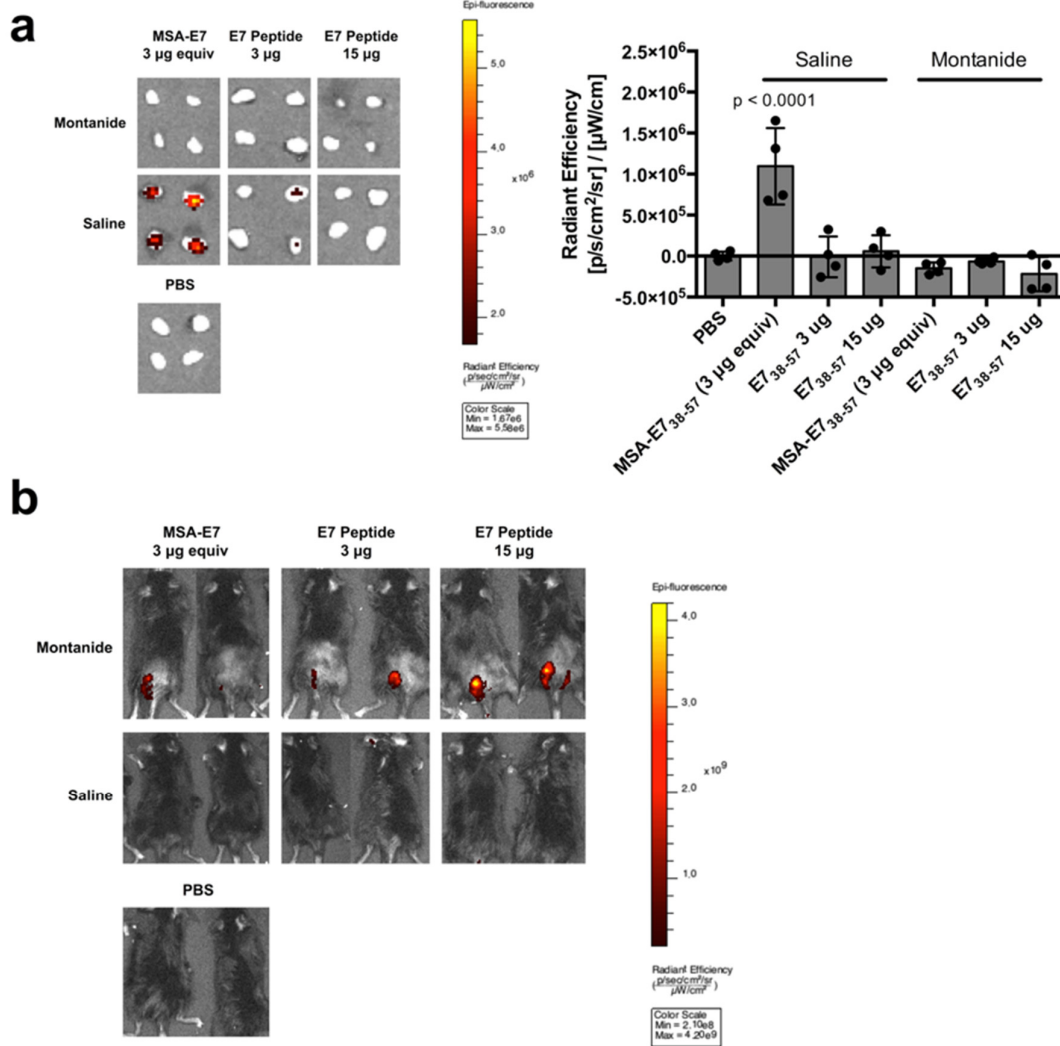
Supplementary Figure 5 Montanide formulation fails to enhance dLN bioavailability **(a,b)** FITC-labeled E7$_{38-57}$ or MSA-E7$_{38-57}$, formulated either in saline or Montanide, was injected subcutaneously in mice at the indicated doses. 8 hours after injection, inguinal lymph nodes (n = 4 lymph nodes per group) **(a)** and injection sites (mean ± SD, n = 2 mice per group) **(b)** were imaged on IVIS. Statistical significance calculated using one-way ANOVA with Dunnett's multiple comparisons test against PBS **(a)**.
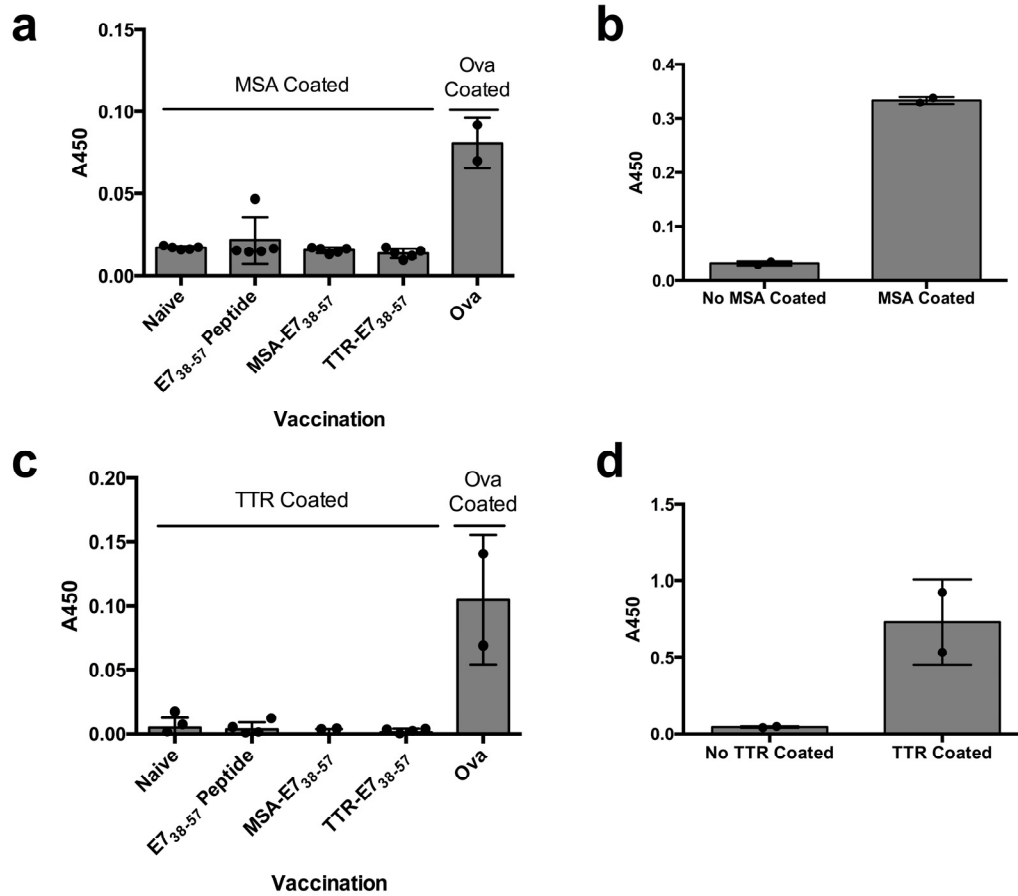
Supplementary Figure 6 No antibody responses are detected against MSA nor TTR following vaccination. **(a,c)** Serum from mice primed and boosted with the indicated vaccine was collected and IgG purified with Protein A resin. The presence of anti-MSA **(a)** or anti-TTR **(c)** antibodies was measured with an ELISA plate coated with the corresponding protein of interest. Following serum incubation and washes, a chicken anti-mouse antibody was used as a detection reagent. Ova vaccinated animals and ova-coated wells were used as positive controls (mean $\pm$ SD, n = 2 mice for Ova controls and n = 5 mice for other groups). **(b,d)** To confirm that MSA- **(b)** and TTR- **(d)** coated wells were of high quality, anti-MSA and anti-TTR antibodies were used as detection reagents (mean $\pm$ SD, n = 2 mice per group).
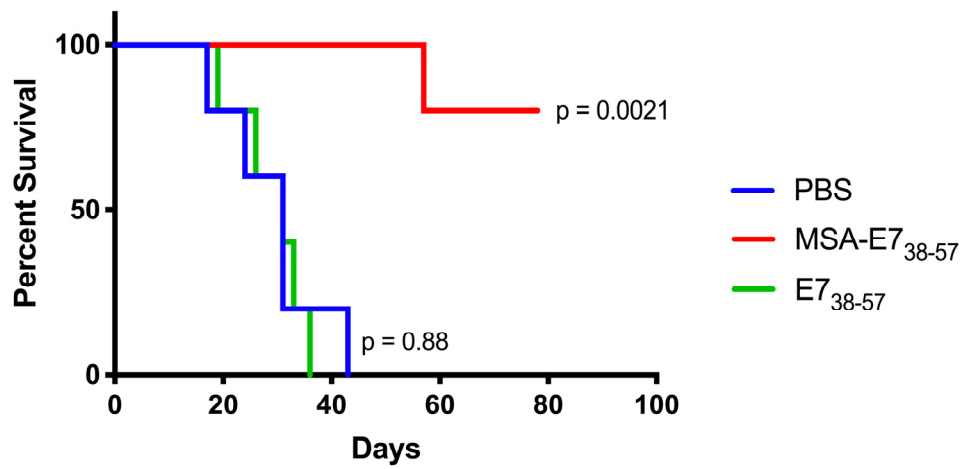
Supplementary Figure 7 MSA-E7$_{38-57}$-vaccinated mice generate anti-E7 memory. 66 days following boost, mice were inoculated with 300k TC-1 cells and euthanized after tumors exceeded 100 mm^2 in area (n = 5 mice per group). Statistical significance calculated using two-tailed long-rank (Mantel-Cox) test versus PBS.
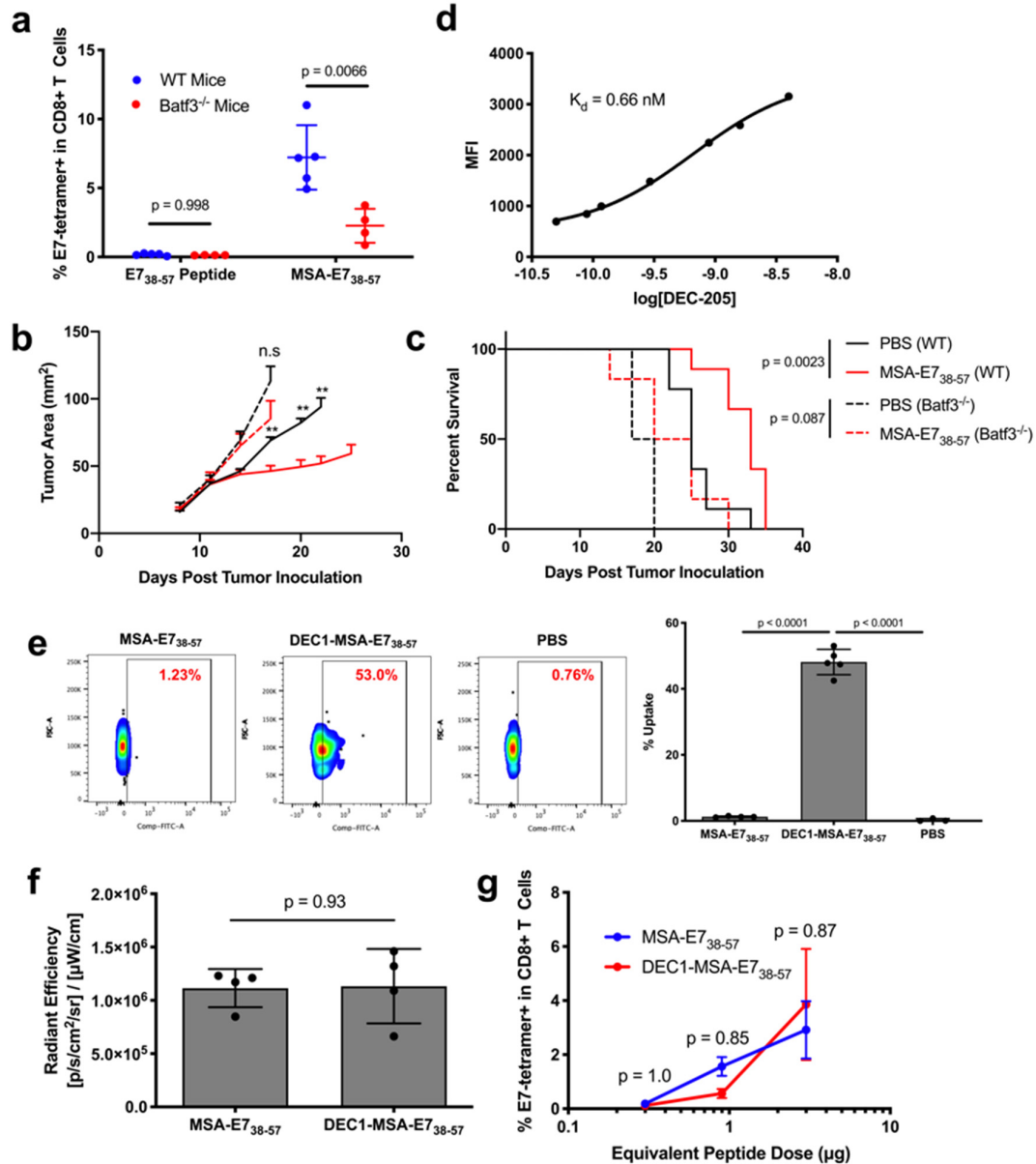
Supplementary Figure 8 Targeting CD8+ DCs fails to enhance MSA-E7$_{38-57}$ immunogenicity. **(a)** Mice (WT or Batf3$^{-/-}$) were primed and boosted with E7$_{38-57}$ or MSA-E7$_{38-57}$ plus CDN subcutaneously. Shown are tetramer stain data among CD8+ T cells 6 days after boost (mean $\pm$ SD, n = 5 WT mice and 4 Batf3$^{-/-}$ mice per group). **(b-c)** WT or Batf3$^{-/-}$ mice were implanted with TC-1 tumors. On days 8 and 15, mice were vaccinated with MSA-E7$_{38-57}$ and CDN or PBS control. Mice were euthanized when tumors reached 100 mm^2 in area. Tumor growth curves are plotted until the first mouse

is euthanized in each group (n = 9 mice for WT conditions and 6 mice for Batf3$^{-/-}$ conditions). Shown are tumor growth curves **(b)** and survival data **(c)**. **(d)** Soluble biotinylated DEC-205 was used to label yeast displaying DEC1 fibronectin, and MFI following secondary incubation was used to calculate the K_d of DEC1. **(e)** AF488-labeled MSA-E7$_{38-57}$ or DEC1-MSA-E7$_{38-57}$ was injected subcutaneously in mice. 24 hours later, the inguinal lymph node was excised and AF488 signal in CD8+ DCs was assessed by flow cytometry (mean ± SD, n = 5 mice per group). **(f)** FITC-labeled MSA-E7$_{38-57}$ or DEC1-MSA-E7$_{38-57}$ was injected subcutaneously in mice. 8 hours later, the inguinal node was imaged by IVIS (mean ± SD, n = 4 lymph nodes per group). **(g)** Mice were primed and boosted with the indicated doses of MSA-E7$_{38-57}$ or DEC1-MSA-E7$_{38-57}$ plus CDN subcutaneously. Shown are tetramer stain data among CD8+ T cells 6 days after boost (mean ± SEM, n = 5 mice per group). Data are representative of three independent experiments. Statistical significance calculated using two-tailed t tests and Holm-Sidak multiple comparisons test within each group **(a,g)** or time-point **(b)** on the x-axis, or without multiple comparisons test **(f)**, by two-tailed log-rank (Mantel-Cox) test versus PBS **(c)**, or by one-way ANOVA with Tukey's multiple comparisons test **(e)**.
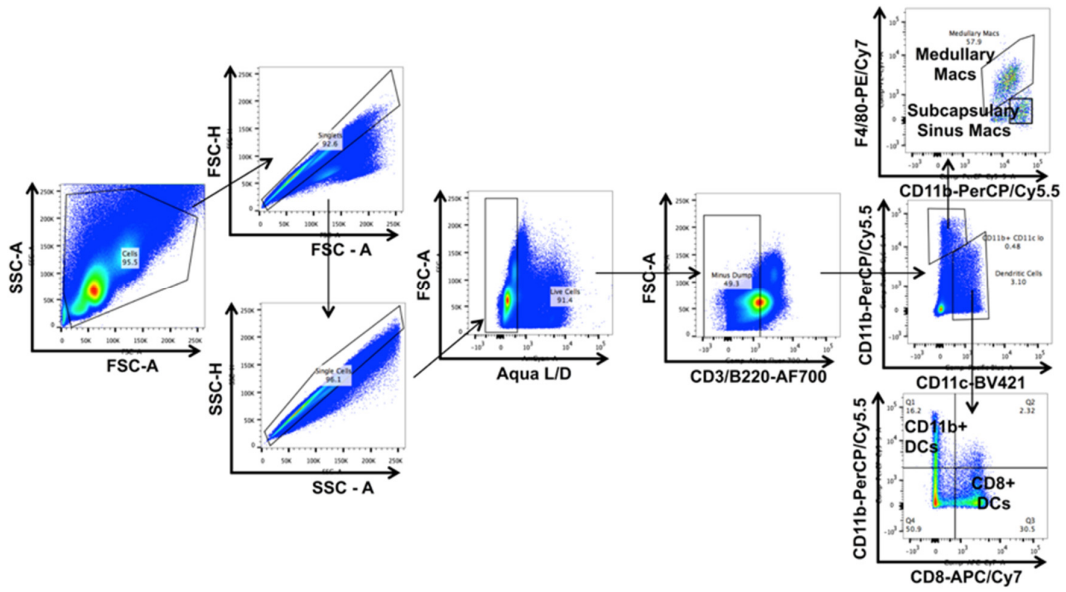
Supplementary Figure 9 Gating scheme to identify antigen presenting cells from digested lymph nodes
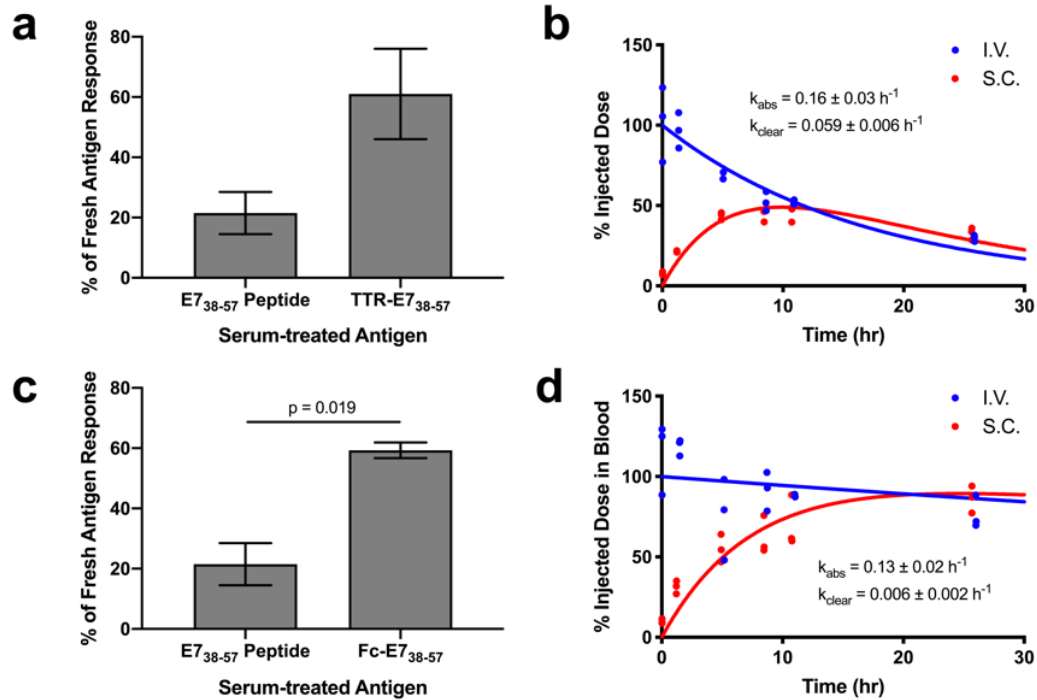
Supplementary Figure 10 TTR- and Fc-E7$_{38-57}$ protect E7$_{38-57}$ from degradation in serum and slow systemic absorption. **(a,c)** Splenocytes from E7$_{38-57}$-vaccinated mice were restimulated in the presence of brefeldin A with indicated antigen, either fresh or treated with 10% mouse serum for 24 hours. Shown is the percentage IFNγ response from serum-treated antigen restimulation compared to response from fresh antigen as measured by intracellular cytokine staining (n = 2 replicates). TTR-E7$_{38-57}$ shown in **(a)** and Fc-E7$_{38-57}$ shown in **(c)**. **(b,d)** FITC labeled TTR-E7$_{38-57}$ **(b)** or Fc-E7$_{38-57}$ **(d)** was injected either subcutaneously or intravenously in mice (fit data ± SE, n = 3 mice per group). 10 µl blood draws were used to quantify antigen concentration in serum over the course of 24 hours following injection; data was used to determine pharmacokinetic model fits, shown with solid lines. Statistical significance calculated with two-tailed t-tests **(a,c)**.
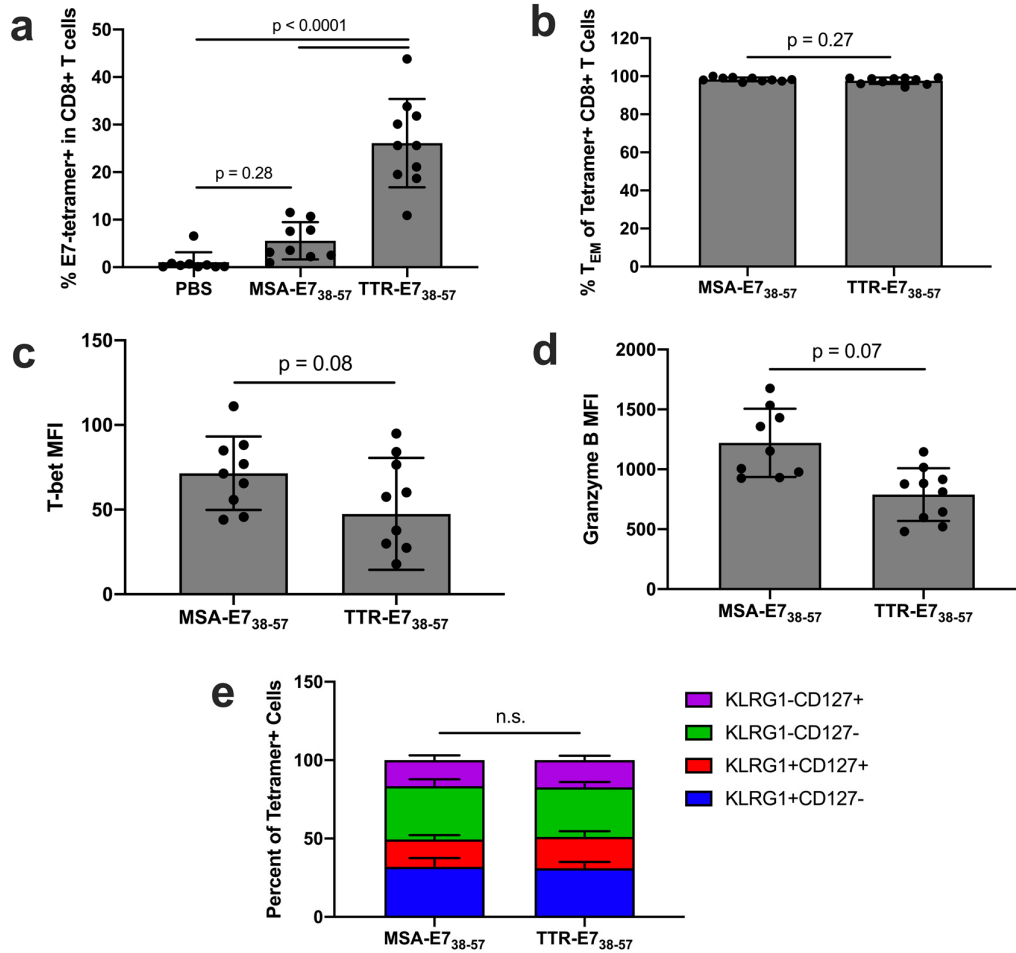
Supplementary Figure 11 TTR-E7$_{38-57}$ vaccination drives a higher magnitude CD8+ T cell response than MSA-E7$_{38-57}$ without modulating T cell immunophenotype. **(a-e)** TC-1 tumor-bearing mice were vaccinated on days 8 and 15 with the indicated vaccine. CD8+ T cells from peripheral blood were analyzed on day 21 (mean ± SD, n = 9 for PBS and MSA-E7$_{38-57}$; n = 10 for TTR-E7$_{38-57}$ throughout). Shown are tetramer stain data **(a)**, and further characterization of the tetramer+ CD8+ T cell population **(b-e)**, including %T$_{EM}$, defined as CD44$^+$CD62L$^-$ **(b)**, expression of T-bet **(c)** and granzyme B **(d)**, and characterization of CD127 and KLRG1 **(e)**. Statistical significance calculated using a one-way **(a)** or two-way **(e)** ANOVA with Tukey's multiple comparisons test between all groups, or with two-tailed t-tests **(b-d)**.
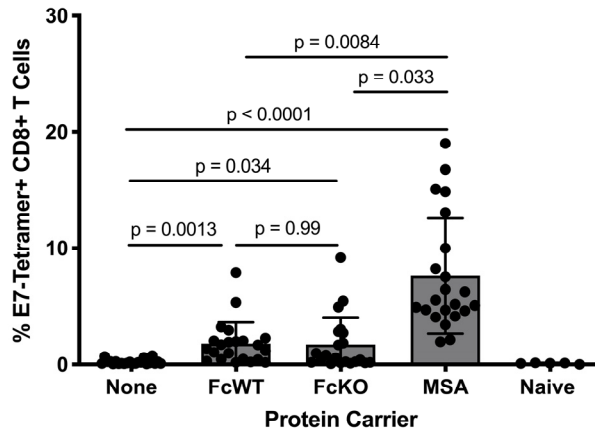
Supplementary Figure 12 Fc-E7$_{38-57}$ efficacy is receptor-independent. Mice were primed and boosted with 3 μg E7$_{38-57}$ or equimolar doses of the indicated protein-E7$_{38-57}$ fusion plus CDN subcutaneously. Shown are tetramer stain data among CD8+ T cells 6 days after boost (mean ± SD, n = 5 mice for naïve controls and 22 mice for all other groups). Data are pooled from four independent experiments. Statistical significance calculated using one-way ANOVA with Tukey's multiple comparisons test.
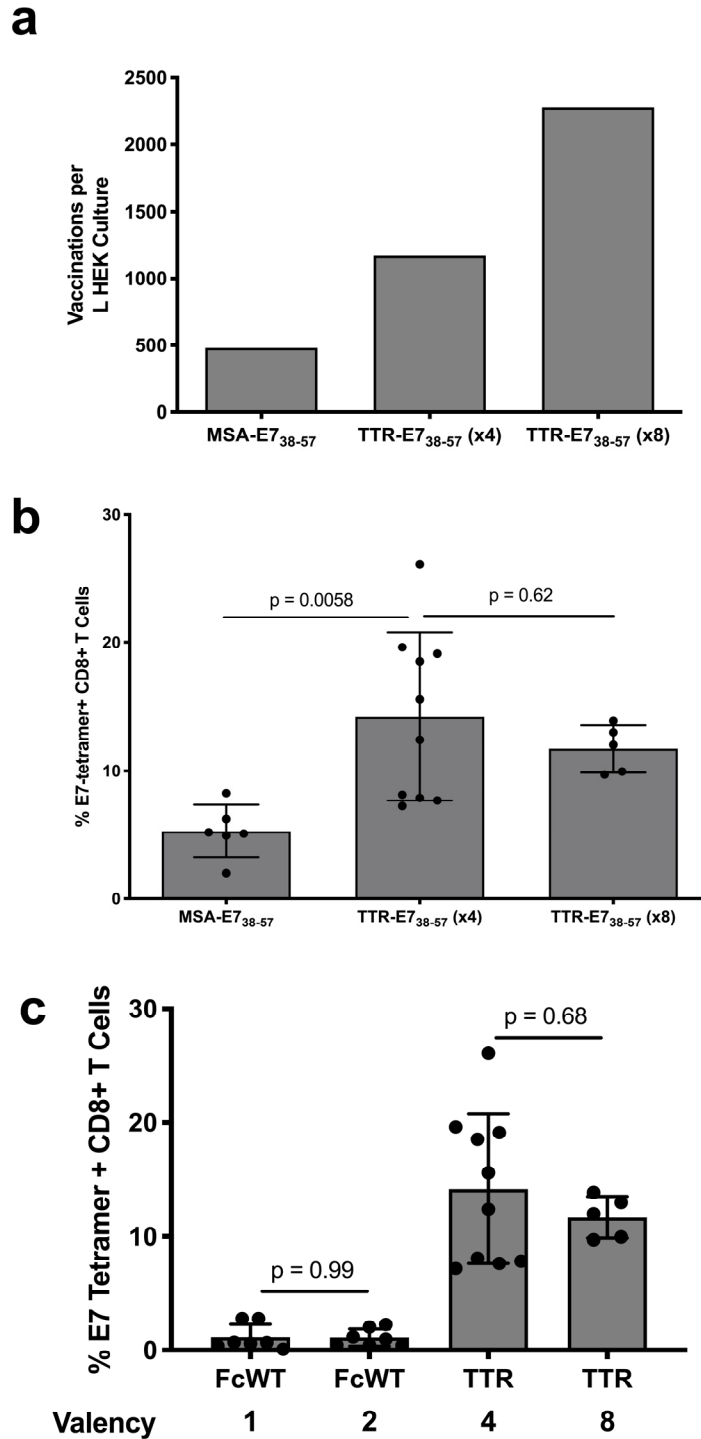
Supplementary Figure 13 TTR-mediated delivery of high-valency antigen. **(a)** Yields from the supernatant of HEK cell culture one week after transfection with the indicated constructs, calculated in terms of numbers of typical 3 μg peptide-equivalent doses of

vaccine per liter of culture. **(b)** Mice were vaccinated with MSA-E7$_{38\text{-}57}$ or TTR-E7$_{38\text{-}57}$ with the indicated E7$_{38\text{-}57}$ copy number. Shown are tetramer stain data 6 days after boost (mean $\pm$ SD, n = 6 mice for MSA-E7$_{38\text{-}57}$, 10 mice for TTR-E7$_{38\text{-}57}$ (valency of 4), and 5 mice for TTR-E7$_{38\text{-}57}$ (valency of 8)). **(c)** Mice were vaccinated with an equimolar amount of E7$_{38\text{-}57}$ in the form of Fc-E7$_{38\text{-}57}$ or TTR-E7$_{38\text{-}57}$ in the indicated copy number. Shown are tetramer stain data 6 day after boost (mean $\pm$ SD, n = 7 mice for both FcWT-E7$_{38\text{-}57}$ vaccines, 10 mice for TTR-E7$_{38\text{-}57}$ (valency of 4), and 5 mice for TTR-E7$_{38\text{-}57}$ (valency of 8). Statistical significance calculated using one-way ANOVA with Tukey's multiple comparisons test **(b)** or two-tailed t tests within each protein carrier category **(c)**.

Figure Panel(s)	Mouse line	Cell line
Figure 1: c-f	C57BL/6	N/A
Figure 2: a-c, e	C57BL/6	N/A
Figure 2: d	C57BL/6	TC-1
Figure 3: a-h	C57BL/6; transferred T cells from pmel Thy1.1[+] mice in panels e-g; transferred T cells from OTI Thy1.1[+] mice in panel h	N/A
Figure 4: a-g, i	C57BL/6; transferred T cells from pmel Thy1.1[+] mice in panels e and f	N/A
Figure 4: h	C57BL/6	TC-1
Figure 5: a, b	C57BL/6	N/A
Figure 5: d-g	C57BL/6	B16F10
Figure 5: h	HLA-A11	N/A
Figure 5: i	HLA-A2	N/A
Supplementary Figure 1: b	C57BL/6	N/A
Supplementary Figure 3: b	Plasma from B57BL/6 mice	N/A
Supplementary Figure 4	OTI Thy1.1[+]	N/A
Supplementary Figure 5: a, b	C57BL/6	N/A
Supplementary Figure 6: a-d	C57BL/6	N/A
Supplementary Figure 7	C57BL/6	TC-1
Supplementary Figure 8: a	Batf3^{-/-} mice, with C57BL/6 as control	N/A
Supplementary Figure 8: b,c	C57BL/6	TC-1
Supplementary Figure 8: e-g	C57BL/6	N/A
Supplementary Figure 9	C57BL/6	N/A
Supplementary Figure 10	C57BL/6	N/A
Supplementary Figure 11	C57BL/6	N/A
Supplementary Figure 12	C57BL/6	TC-1
Supplementary Figure 13: b,c	C57BL/6	N/A

Supplementary Table 1 Mouse strains and cell lines used in each figure

Component	Amino Acid Sequence
Fc (IgG2c)	EPRVPITQNPCPPLKECPPCAAPDLLGGPSVFIFPPKIKDVLMI SLSPMVTCVVVDVSEDDPDVQISWFVNNVEVHTAQTQTHR EDYNSTLRVVSALPIQHQDWMSGKEFKCKVNNRALPSPIEK TISKPRGPVRAPQVYVLPPPAEEMTKKEFSLTCMITGFLPAEI AVDWTSNGRTEQNYKNTATVLDSDGSYFMYSKLRVQKST WERGSLFACSVVHEGLHNHLTTKTISRSLGK
MSA	EAHKSEIAHRYNDLGEQHFKGLVLIAFSQYLQKCSYDEHAK LVQEVTDFAKTCVADESAANCDKSLHTLFGDKLCAIPNLRE NYGELADCCTKQEPERNECFLQHKDDNPSLPPFERPEAEAM CTSFKENPTTFMGHYLHEVARRHPYFYAPELLYYAEQYNEI LTQCCAEADKESCLTPKLDGVKEKALVSSVRQRMKCSSMQ KFGERAFKAWAVARLSQTFPNADFAEITKLATDLTKVNKEC CHGDLLECADDRAELAKYMCENQATISSKLQTCCDKPLLK KAHCLSEVEHDTMPADLPAIAADFVEDQEVCKNYAEAKDV FLGTFLYEYSRRHPDYSVSLLLRLAKKYEATLEKCCAEANP PACYGTVLAEFQPLVEEPKNLVKTNCDLYEKLGEYGFQNAI LVRYTQKAPQVSTPTLVEAARNLGRVGTKCCTLPEDQRLPC VEDYLSAILNRVCLLHEKTPVSEHVTKCCSGSLVERRPCFSA LTVDETYVPKEFKAETFTFHSDICTLPEKEKQIKKQTALAEL VKHKPKATAEQLKTVMDDFAQFLDTCCKAADKDTCFSTEG PNLVTRCKDALA
TTR	GPAGAGESKCPLMVKVLDAVRGSPAVDVAVKVFKKTSEGS WEPFASGKTAESGELHGLTTDEKFVEGVYRVELDTKSYWK TLGISPFHEFADVVFTANDSGHRHYTIAALLSPYSYSTTAVV SNPQN
DEC1	VSDVPRDLEVAAATPTSLLISWRSTPYAAYYRITYGETGGNS PVQEFTVPRSASSATISGLKPGVDYTIAAYAVTWTGYPLPISI NYRTEIDKPSQGS
Linker	GGGS
E7$_{38-57}$	IDGPAGQAEPDRAHYNIVTF
Trp1$_{1455-63}$ APL	TAPDNLGYM
gp100$_{20-39}$ APL	AVGALEGPRNQDWLGVPRQL
CEA$_{567-84}$	RAYVSGIQNSVSANRSDP
Ova$_{251-270}$	GLEQLESIINFEKLTEWTSS
Kras$_{2-21,G12D}$	TEYKLVVVGADGVGKSALTI
H3.3$_{21-40,K27M}$	ATKAARMSAPSTGGVKKPHR
His Tag	HHHHHH

Supplementary Table 2 Protein sequences. Protein fusions take the form: protein – linker – epitope – linker – His tag; targeting domain – linker – protein – linker – epitope; or protein – linker – epitope 1 – linker – epitope 2 – linker – His tag

List of abbreviations

ACK - ammonium chloride potassium

ANOVA - analysis of variance

APC - antigen presenting cell

APL - altered peptide ligand

AUC - area under the curve

BSA - bovine serum albumin

CDN - cyclic di-nucleotide

CFSE - carboxyfluorescein succinimidyl ester

dLN - draining lymph node

DLS - dynamic light scattering

EDTA - ethylenediaminetetraacetic acid

ELISA - enzyme-linked immunosorbent assay

ELISPOT - enzyme-linked immune absorbent spot

FITC - fluorescein isothiocyanate

HEK - human embryonic kidney

HMW - high molecular weight

ICS - intracellular cytokine staining

IFN - interferon

IVIS - in vivo imaging system

KLH - keyhole limpet hemocyanin

MFI - mean fluorescence intensity

MSA - mouse serum albumin

PBMC - peripheral blood mononuclear cells

PBS - phosphate-buffered saline

PK - pharmacokinetic

SEC - size exclusion chromatography

SEM - standard error of the mean

STING - stimulator of interferon genes

TLR - Toll-like receptor

TMB - 3,3',5,5'-Tetramethylbenzidine

TNF - tumor necrosis factor

TTR - transthyretin